Discover Mechanical Engineering

Discover

Brief Communication

Enhancement of laser cut edge quality of ultra-thin titanium grade 2 sheets by applying an in-process approach using modulated Yb:YAG continuous wave fiber laser

Alexander Bartsch[1,3,4] · Moritz Burger[1,3,4] · Marius Grad[2] · Lukas Esper[2] · Ulrich Schultheiß[3] · Ulf Noster[2] · Thomas Schratzenstaller[1,3,4]

Received: 6 April 2023 / Accepted: 20 June 2023
Published online: 03 July 2023

Abstract
Titanium is used in many areas due to its excellent mechanical, biological and corrosion-resistant properties. Implants often have thin and filigree structures, providing an ideal application for fine cutting with laser. In the literature, the main focus is primarily on investigating and optimizing the parameters for titanium sheets with thicknesses greater than 1 mm. Hence, in this study, the basic manufacturing parameters of laser power, cutting speed and laser pulse of a 200 W modulated fiber laser are investigated for 0.15 mm thick grade 2 titanium sheets. A reproducible, continuous cut could be achieved using 90 W laser-power and 2 mm/s cutting-speed. Pulse pause variations between 85 and 335 µs in 50 µs steps and a fixed pulse width of 50 µs show that a minimum kerf width of 23.4 µm, as well as a minimum cut edge roughness Rz of 3.59 µm, is achieved at the lowest pulse pause duration. An increase in roughness towards the laser exit side, independent of the laser pulse pause duration, was found and discussed. The results provide initial process parameters for cutting thin titanium sheets and thus provide the basis for further investigations, such as the influence of cutting gas pressure and composition on the cut edge.

Keywords Laser cutting · Titanium sheet · Kerf

1 Introduction

Titanium has long been used for a wide range of high-performance products. In the aerospace and marine sectors, but also in medical technology, the material has established itself due to its superior properties compared to other metallic materials [1–4]. It has a high strength-to-weight ratio, good resistance to fatigue and corrosion, and good biocompatibility [5, 6].

But compared to other established engineering materials such as stainless steel, titanium is difficult to machine using conventional methods such as milling, turning, grinding, and drilling. This is due to its low modulus of elasticity

Alexander Bartsch and Moritz Burger contributed equally to this work.

✉ Alexander Bartsch, alexander.bartsch@oth-regensburg.de; Moritz Burger, moritz.burger@oth-regensburg.de; Marius Grad, marius.grad@oth-regensburg.de; Lukas Esper, lukas.esper@oth-regensburg.de; Ulrich Schultheiß, ulrich.schultheiss@oth-regensburg.de; Ulf Noster, Ulf.Noster@oth-regensburg.de; Thomas Schratzenstaller, Thomas.Schratzenstaller@oth-regensburg.de | [1]Medical Device Lab, OTH Regensburg, Regensburg, Germany. [2]Material Science and Surface Analytic Lab, OTH Regensburg, Regensburg, Germany. [3]Regensburg Center of Health Sciences and Technology (RCHST), OTH Regensburg, Regensburg, Germany. [4]Regensburg Center of Biomedical Engineering (RCBE), OTH Regensburg, Regensburg, Germany.

($E_{Titanium}$ = 105 GPa), low thermal conductivity (11.4 W/mK), and strong chemical activity at elevated temperatures [2, 3, 6]. Since laser cutting does not cause heating due to friction, the heat input is very localized and chemical reactions can be prevented by using an inert gas atmosphere. Laser cutting is suitable as a non-contact manufacturing process for titanium [2] and the high tool wear that occurs, for example, when milling titanium can thus be avoided. In addition, laser cutting is ideal for the economical production of filigree structures due to its speed, precision, and resource efficiency [2, 7].

A variety of devices are cut with lasers from a thin base material, e.g. in medical applications for coronary stents or osteosynthesis plates. The requirements for the quality of the laser cut are high in medical technology. This is due to the influence of the cutting edge on biocompatibility, the legal and standard requirements (EN ISO 9013:2000) and the filigree structures, e.g. a structure width of approx. 80 µm for stents [1, 8–10] Thus, in the development of minimally invasive implants, which are often manufactured in a (partially) unexpanded form—such as stents or orbital floor implants (implanted via the maxillary sinus)—the implant struts are very close together and a too large laser kerf would limit the design freedom of the implant. Therefore, it is necessary that finest elements can be cut from the material. For this purpose, a minimal kerf is required. To meet these requirements, it is necessary to use an inert cutting gas, such as argon. This is intended to prevent an enrichment of nitrogen and oxygen and prevent the formation of microcracks in the cutting area [1, 2, 7–9, 11].

The influence of the cutting parameters on the kerf during laser cutting has already been investigated for many materials used in medical technology with a sheet thickness below 1 mm [12]. In the case of titanium, previous investigations mainly refer to sheet thicknesses greater than 1 mm or do not give any specific parameters for sheet thicknesses less than 1 mm [2, 3, 7, 8, 11, 13–21]. The ideal process parameters found are difficult to transfer to thinner sheet thicknesses because, for example, the necessary laser power, cutting speed, gas pressure, etc. depend strongly and non-linearly on the material thickness to be cut [22–24]. Even though ultrashort pulse lasers show a better result in terms of cut quality [12], they are still expensive and therefore not available for all users. Fiber lasers such as Nd:YAG or Yb:YAG are cheaper and widely used, especially in industry.

Another important property in implants is surface roughness. Surface roughness can affect various properties of the implant. These include surface wettability, cell interaction, and mechanical behavior of the implant [25]. Surface roughness can be divided into the following groups: Macro-roughness (> 100 µm), Micro-roughness (100 nm–100 µm) and Nano-roughness (< 100 nm). The response of cells to the implant can be affected by each group [26]. For implants, roughness values of Ra < 8 µm have been shown to be useable [27]. Some publications indicate that values as low as Ra < 25 µm can be used [25].

Thus, this work focuses on laser fine cutting of grade 2 titanium sheets with a material thickness of 0.15 mm using a fiber laser. The parameters investigated are the laser power, cutting speed and a suitable ratio between laser pulse and pause duration (laser duty cycle at fixed pulse width), since these parameters have a great influence on the cutting edge roughness and a reproducible and minimal kerf in thin titanium sheets [8, 9, 13, 28]. It is expected that as the laser duty cycle increases and the laser power increases, it will be possible to successfully cut faster [9, 23]. At higher cutting speeds, the roughness of the cutting edge is likely to decrease [24].

2 Material and methods

The investigated sheets of grade 2 titanium have a thickness of 0.15 mm. The chemical analysis of the material is presented in Table 1a and the mechanical properties in Table 1b. The data are based on the manufacturer's specifications for the sheet metal and were additionally validated by spark spectroscopy measurements. The sheets were not cleaned before or between investigations. This is because the results of the tests should yield parameters that make it possible to dispense with pre-treatment and post-treatment as far as possible.

The laser system used was a 200 W TruFiber 200P compact (Trumpf SE & Co. KG, Ditzingen, Germany) fiber laser in modulated continuous wave (CW) mode with ytterbium-doped yttrium aluminium garnet (YAG) as the active medium. The wavelength of the laser was 1068–1072 nm with a beam quality of BPP = 0.38 ± 0.03 mm * mmrad, which translates to a Diffraction index of M^2 = 1.03–1.21. Raw beam diameter after collimation is 5 mm. The cutting head (Precitec GmbH & Co. KG, Gaggenau-Bad Rotenfels, Germany) has a 50 mm focal length, as well as an internal cutting gas supply to the Ø 0.2 mm cutting nozzle. The distance between the nozzle and the surface of the sample is 0.2 mm. The theoretical size of

Table 1 Properties of the investigated grade 2 titanium sheets

(a) Chemical analysis of the investigated grade 2 titanium sheets	
Element	Analysis wt %
Fe	0.042
C	0.012
N	0.003
H	0.001
O	0.1
Ti	Rest/balance
(b) Mechanical properties of the investigated grade 2 titanium sheets	
Mechanical properties	Value
Tensile strength [MPa]	433
Yield strength [MPa]	286
Elongation	33
Surface roughness (Sz) [µm]	5.7 ± 1.7

the laser spot (d_{Spot}) is 16 µm. The maximum BBP/M^2 value of the laser manufacturer was used for the calculation shown in Eq. 1. This is therefore a worst-case consideration.

$$d_{laserspot} = \frac{4 \cdot \lambda \cdot f \cdot M^2}{\pi \cdot d_{raw}} = 16.48\,\mu\text{m} \tag{1}$$

where λ is the wave length of the laser; f is the focal length; M^2 is the beam propagation ratio; d_{raw} is the raw beam diameter.

The focus position of the laser was adjusted to the middle of the sheet thickness. All tests were carried out with 10 bar argon 5.0 cutting gas pressure—measured at the cutting nozzle. The cutting gas pressure corresponded to a flow rate of 30 l/min. The cutting table used was an ATS100 two axis traverse table (Aerotech GmbH, Fürth, Germany) with a repeatability of ± 0.3 µm and accuracy of ± 9 µm. The laser cutting setup is shown in Fig. 1.

The laser scanning microscope measurements were performed with an Olympus Lext 3D Measuring Laser Microscope OLS400 (Olympus Europa SE & Co. KG, Hamburg, Germany) with a laser wavelength of 400–420 nm. The cut-off distance λ_c for the roughness measurements was 80 µm.

In Fig. 2a, the laser cutting process with an internal cutting gas supply is shown schematically. It can be seen how the molten material is ejected downwards through the cutting gas flow. The resulting kerf with its characteristic shape and area of influence known as the heat-affected zone (HAZ), is shown in Fig. 2b.

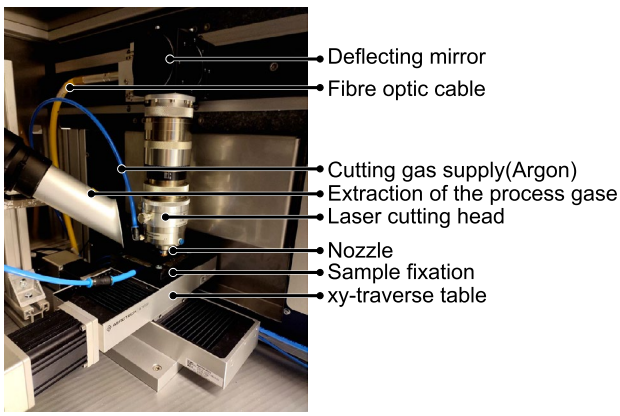

Fig. 1 Illustration of the laser cutting system used

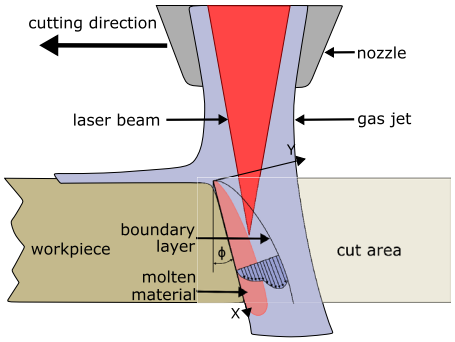

(a) Schematic laser cutting process with an internal cutting gas supply (adapted from [29])

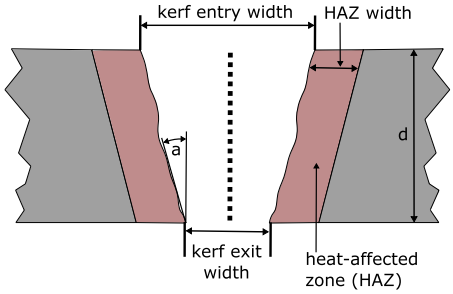

(b) Resulting characteristic kerf after laser cutting (adapted from [30])

Fig. 2 Schematic representation of most relevant aspects and effects associated with laser cutting

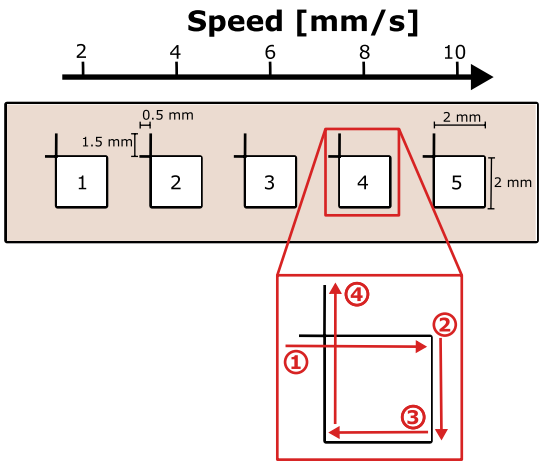

Fig. 3 Quadratic cutting pattern with applied cutting sequence of the laser at a constant power level and variation of the cutting speed; entry and exit lanes of the laser are shown for the acceleration of the two axis traverse table, as well as the laser switch-on delay

In the first step of the investigation, a process window must be found in which a square cutting pattern (see Fig. 3) can be reliably and continuously cut and detached from the sheet without much mechanical effort. To make the mechanical effort reproducible and automatable, an ultrasonic bath is used.

The cutting speed is varied (2–10 mm/s) for each selected laser power level (50–120 W in 10 W steps). Subsequently, the cut samples were placed in an ultrasonic bath, Sonorex Super RK 102H (BANDELIN electronic GmbH & Co. KG, Berlin, Germany); containing 350 ml deionised water; and 30 ml ethanol for 5 min.

The samples remained freely immersed in the medium and had no wall contact in the ultrasonic bath before detaching from the sheet. A cut is considered complete and successful when the cut square has detached from the sheet only due to the ultrasonic vibration. With the identified parameters of power and cutting speed, a process window for a reproducible, continuous laser cut could be found. Since the laser system is limited to a minimum pulse duration of 50 µs and shorter pulses are useful to achieve better results, the pulse duration is kept constant at 50 µs. To investigate the influence of the laser duty cycle on the width and roughness of the kerf despite a constant low pulse duration, the pulse duration is kept constant but the period duration is increased. Therefore, the laser pause duration is used as a variable. For this purpose, the sample geometry shown in Fig. 4 was cut with the previously determined power.

The period duration is increased in 50 µs steps. Here, the investigation covers a period duration between 135 µs and 385 µs. Each sample contains five open and five closed laser cuts. For the open laser cuts, the opposing material is not part of the sample, but for the closed laser cut it is. These are thus closed and open kerf gaps, respectively. For the open kerf gaps, kerf gap roughness (Ra, Rz) and for the closed kerf gaps, kerf gap width were investigated using a confocal laser scanning microscopy (CLSM). The roughness measurements were taken along the kerf in four different planes parallel to the sheet surface. The first measurement was taken 8 µm below the sheet surface as seen from the laser entry side. The other measurements were taken at an incremental distance of 40 µm below (measurement positions schematically shown in Fig. 4). The width of the kerf was measured with the same device from the beam entry side.

All experiments and investigated parameters are listed in Table 2.

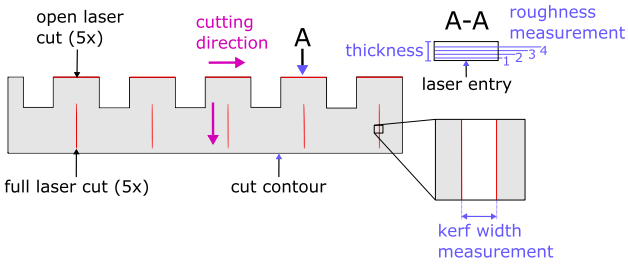

Fig. 4 Sample geometry for the investigation of laser pulsing on kerf width and roughness

Table 2 Overview of all tests performed

Tested parameter(s)	Laser power and cutting speed	Laser cycle duration with fixed 50 µs pulse duration
Range of para- meter variation	50–120 W in 10 W steps under variation of cutting speed (2–10 mm/s in 2 mm/s steps)	85–335 µs pulse duration with 50 µs pulse width
Number of samples	4 of each power and cutting speed setting	15 open and closed cutting edges per pulse variation

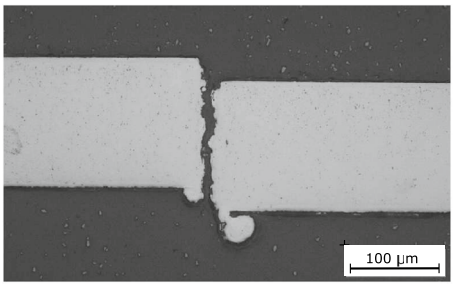

(a) Embedded micrograph through a laser cut square (on the right side) at a laser power of 70 W and 10 mm/s. At this cut plane, the material has clearly been successfully cut through. Nevertheless, during treatment in the ultrasonic bath, it did not detach. As described in the text, this is due to wedging of the opposite sides of the ultra-thin titanium sheet.

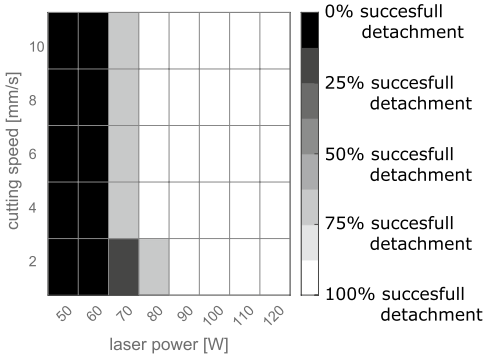

(b) Successful detachment in ultrasonic bath of cut squares as a criterion for a valid laser cut

Fig. 5 Analysis of cutting kerf under variation of cutting speed and laser power

3 Results and discussion

3.1 Variation of laser power and cutting speed

The combination of laser power and cutting speed was varied from 50–120 W and 2–10 mm/s, respectively. The quadratic cut patterns were treated with ultrasonic bath and it was determined whether the squares could be detached by this treatment. This serves as proof that the kerf is sufficiently large and continuous. Unsuitable cutting parameters lead to wedging of the opposite sides of the ultra-thin titanium sheet, which makes it difficult to detach the cut squares, as shown in Fig. 5a.

Figure 5b shows, as the laser power increases, the probability of detachment increases. As the cutting speed increases, the easiness of detachment increases also.

One possible explanation of this fact is: the lower the cutting speed, the more heat is introduced into the cutting geometry. At a laser power of at least 90 W, all squares became detached, regardless of the cutting speed. This power was assessed as sufficient and used for the further investigations. Also, this additional heat input could lead to an unintended change in the microstructure [2, 31]. In addition, at a higher cutting speed, less time is required for a given cut length, which is highly important in terms of economic aspects. The most suitable parameters for the following results are a laser power of 90 W and a cutting speed of 10 mm/s.

3.2 Variation of the pulse pause

Figure 6 shows the influence of the pulse pause at a fixed pulse duration (50 µs) on the width of the kerf.

The theoretical minimum laser spot size of the laser system of 16 µm is also shown. The kerf width increases with increasing pulse pause duration. The minimum kerf width of 23.4 µm is reached at the lowest investigated pulse pause of 85 µs. This corresponds to a deviation from the theoretical spot size by almost 46%. When the energy of the laser is coupled into the material, areas that were not directly exposed are also heated and liquefied, which is why the actual kerf is always larger than the larger pulse gap, allows the thermal energy of the molten material to be partially transferred to the adjacent area, which in turn also leads to a melting of this area. These two effects influence each other, but each leads to an increase in kerf width. The maximum kerf width of 30.2 µm, as displayed in Fig. 6 found, was achieved with a pulse pause of 285 µs. The displayed roughness values in Fig. 7 are the average of four measurements at different profile depths which are schematically shown in Fig. 4. It can be observed that at the shortest pulse pause duration of 85 µs, a minimum roughness Rz of 4.98 ± 0.40 µm and Ra of 0.8 ± 0.08 µm could be achieved.

Figure 8 shows that the cutting edge roughness increases from the laser entrance to the laser exit side, independent of the pulse pause duration. The line roughness (Ra and Rz) was measured along the kerf. Noticeably, for pulse durations of 85 µs and 135 µs, the lowest roughness Rz of 3.59 µm and 3.44 µm were measured at a distance of 8 µm from the top of the sheet. For longer pulse pauses, higher roughness of $Rz < 4.50$ µm are observed at similar locations.

The measured Rz values increase for all pulse pause durations with increasing measurement depth from the laser entrance side. This correlation can be observed in Fig. 9, where the presence of slag and molten material is shown using 185 µs pulse pause as an example. With pulse durations of 135 µs or shorter, the pause between two pulses is just small enough to ensure that the coupled power density and the associated temperature increase are sufficient to constantly liquefy the material near the surface. This state of aggregation promotes expulsion of molten material and thus lowers the surface roughness. At higher pulse pause durations, as well as in areas of the titanium sheet far from the surface, the coupled power density and the resulting temperature increase of the material are not sufficient to ensure constant liquefaction. This means that between the pulses, the melt in the kerf could partially solidify and then liquefy again with the arrival of the next pulse. On the edge of the cut, splatters can be seen against the direction of the cut. The formation of these can be explained in two ways. A partially-liquefied melted material offers such great resistance to the argon flow that it is dispersed when it is expelled, or else a liquid melted material meets a solid resistance and is dispersed by it. This can explain the increased surface roughness and the structural formations in Fig. 9.

The values achieved for the surface roughness of the kerf can be used in medical technology. For fine bone implants such as the orbital implant mentioned previously, the surface quality is suitable ($Ra < 8$ µm). Here, slag residues could be removed via vibratory grinding, but post-treatment of the kerf surfaces apart from cleaning is not mandatory.

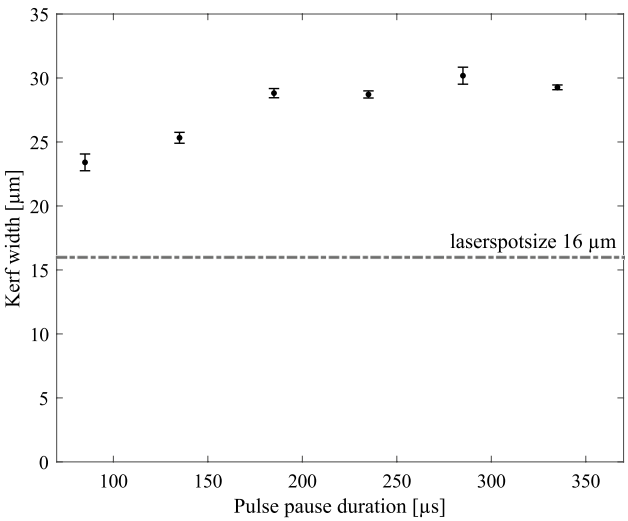

Fig. 6 Influence of the laser pulse pause on kerf width; the theoretical laser spot size of the laser system used is 16 µm

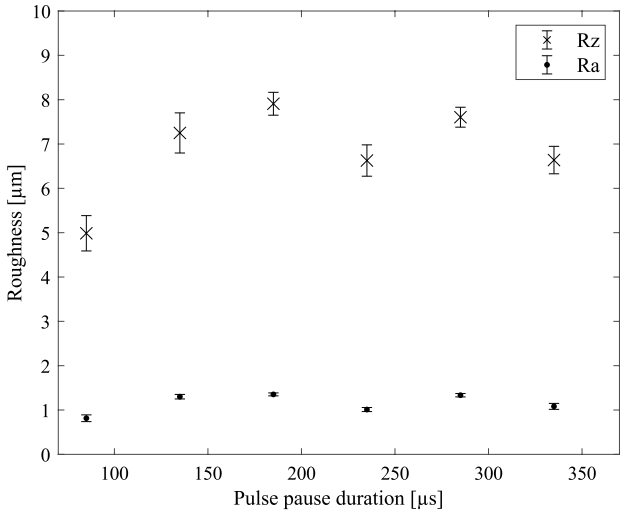

Fig. 7 Cutting edge roughness for different pulse pause durations

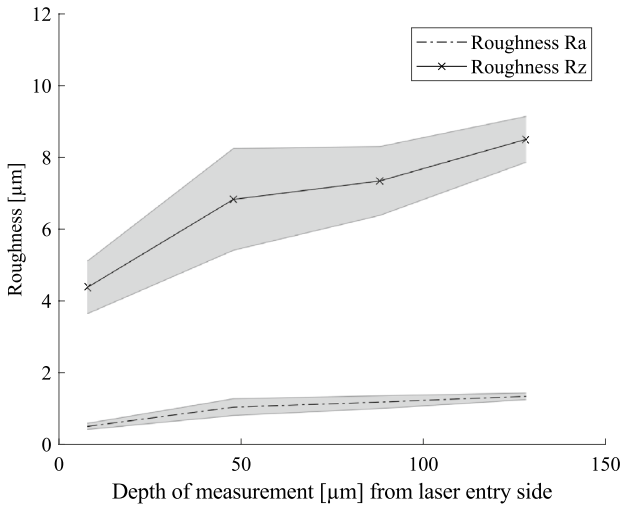

Fig. 8 Cutting edge roughness measured from laser entry to laser exit side

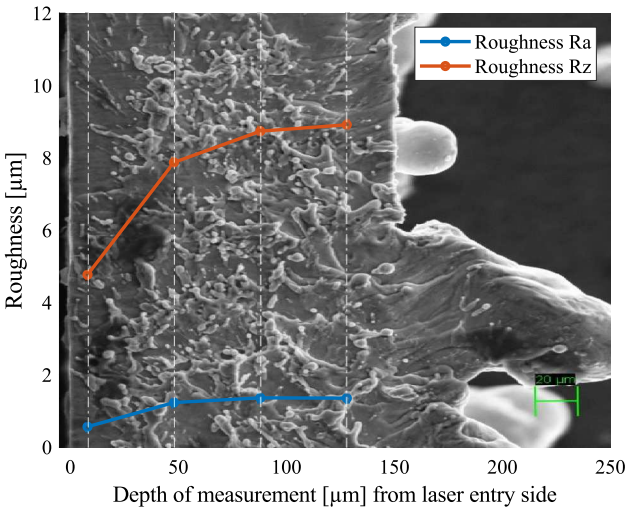

Fig. 9 Measurement of kerf roughness at different distances from the laser entrance side (left) at a pulse pause duration of 185 µs; increasing dross adhesion towards the laser exit side increases kerf roughness values

4 Conclusions

For industrial laser cutting of small structures, a minimum cutting gap is necessary. To achieve this, the following findings were obtained in this work:

- With a laser power of at least 80 W and a cutting speed of 10 mm/s, reproducible, continuous cuts of square shapes in 0.15 mm thick grade 2 titanium sheets could be achieved
- The minimum cutting gap of 23.4 µm was achieved with a pulse pause of 85 µs and a pulse duration of 50 µs
- The kerf width increases with lower laser duty cycle
- The minimum cutting edge roughness of 4.98 ± 0.40 µm of the kerf surface in average was achieved with a pulse pause duration of 85 µs
- For fine bone implants such as the orbital implant mentioned previously, the surface quality is suitable

It should also be noted that the resulting burr at the cut edges still requires post-processing, depending on the quality requirements of the end product. Even at lower laser powers, which were identified as insufficient in this article, ultra-thin titanium sheets could be cut with a suitable post-treatment strategy. This post-processing should be taken into consideration when optimizing the cutting edges, and should be the focus of further work.

Acknowledgements The authors acknowledge the support of Jan Zentgraf and Philipp Lulla (Medical Device Lab, OTH Regensburg, Regensburg, Germany) for their insight and feedback on this publication, as well as Anna Koffler (Medical Device Lab, OTH Regensburg, Regensburg, Germany) for her help with laser-scanning and light microscopy imaging. We would also like to express our special thanks to Prof. Monkman (OTH Regensburg), who was a great help to us with his experience and his English-speaking expertise. Research grant/project "OrbitaTreat" by the Bayerische Forschungsstiftung (BFS); Funding Nr. AZ-1369-19. Regensburg Center of Health Sciences and Technology (RCHST) and Regensburg Center of Biomedical Engineering (RCBE).

Author contributions MB: concept, sample preparation, data processing, writing, editing. AB: concept, sample preparation, data processing, writing, editing. MG: writing, editing, sample analysis (LSM). LE: sample preparation, data processing, editing, graphics. US: sample preparation, SEM analysis, editing. UN: editing, article preparation, proofreading. TS: concept, editing, proofreading.

Funding Open Access funding enabled and organized by Projekt DEAL. Research grant/project *OrbitaTreat* by the Bayerische Forschungsstiftung (BFS); Funding Nr. AZ-1369-19. Regensburg Center of Health Sciences and Technology (RCHST) and Regensburg Center of Biomedical Engineering (RCBE).

Data availability The complete data can be made available upon request.

Code availability Not applicable.

Declarations

Competing interests The authors report there are no competing interests to declare

References

1. Mukherjee S, Dhara S, Saha P. Laser surface remelting of Ti and its alloys for improving surface biocompatibility of orthopaedic implants. Mater Technol. 2018;33(2):106–18. https://doi.org/10.1080/10667857.2017.1390931.
2. Scintilla LD, Sorgente D, Tricarico L. Experimental investigation on fiber laser cutting of Ti6AL4V thin sheet. Adv Mater Res. 2011;264–265:1281–6. https://doi.org/10.4028/www.scientific.net/AMR.264-265.1281.
3. Shrivastava PK, Pandey AK. Multi-objective optimization of cutting parameters during laser cutting of titanium alloy sheet using hybrid approach of genetic algorithm and multiple regression analysis. Mater Today Proc. 2018;5(11):24710–9. https://doi.org/10.1016/j.matpr.2018.10.269.

4. Thakre PR, Singh RP, Slipher G, editors. Mechanics of composite, hybrid and multifunctional materials. In: Conference proceedings of the society for experimental mechanics series, vol. 5. Cham: Springer; 2019.
5. Kaur M, Singh K. Review on titanium and titanium based alloys as biomaterials for orthopaedic applications. Mater Sci Eng C. 2019;102:844–62. https://doi.org/10.1016/j.msec.2019.04.064.
6. Niinomi M, Liu Y, Nakai M, Liu H, Li H. Biomedical titanium alloys with Young's moduli close to that of cortical bone. Regener Biomater. 2016;3(3):173–85. https://doi.org/10.1093/rb/rbw016.
7. Yilbas BS, Shaukat MM, Ashraf F. Laser cutting of various materials: kerf width size analysis and life cycle assessment of cutting process. Opt Laser Technol. 2017;93:67–73. https://doi.org/10.1016/j.optlastec.2017.02.014.
8. Pandey AK, Dubey AK. Modeling and optimization of kerf taper and surface roughness in laser cutting of titanium alloy sheet. J Mech Sci Technol. 2013;27(7):2115–24. https://doi.org/10.1007/s12206-013-0527-7.
9. Rao BT, Kaul R, Tiwari P, Nath AK. Inert gas cutting of titanium sheet with pulsed mode CO2 laser. Opt Lasers Eng. 2005;43(12):1330–48. https://doi.org/10.1016/j.optlaseng.2004.12.009.
10. Wiesent L, Schultheiß U, Schmid C, Schratzenstaller T, Nonn A. Experimentally validated simulation of coronary stents considering different dogboning ratios and asymmetric stent positioning. PLoS ONE. 2019;14(10):0224026. https://doi.org/10.1371/journal.pone.0224026.
11. Pramanik D, Kuar AS, Sarkar S, Mitra S. Enhancement of sawing strategy of multiple surface quality characteristics in low power fiber laser micro cutting process on titanium alloy sheet. Opt Laser Technol. 2020;122: 105847. https://doi.org/10.1016/j.optlastec.2019.105847.
12. Muhammad N, Al Bakri Abdullah MM, Saleh MS, Li L. Laser cutting of coronary stents: progress and development in laser based stent cutting technology. Key Eng Mater. 2015;660:345–50. https://doi.org/10.4028/www.scientific.net/KEM.660.345.
13. Anghel C, Gupta K, Mashamba A. Recent developments in laser cutting of metallic materials, Pretoria/Johannesburg, South Africa (October 29–November 1, 2018). http://ieomsociety.org/southafrica2018/papers/249.pdf.
14. Boudjemline A, Boujelbene M, Bayraktar E. Surface quality of Ti-6AL-4V titanium alloy parts machined by laser cutting. Eng Technol Appl Sci Res. 2020;10(4):6062–7. https://doi.org/10.48084/etasr.3719.
15. Boujelbene M, El Aoud B, Bayraktar E, Elbadawi I, Chaudhry I, Khaliq A, Ayyaz A, Elleuch Z. Effect of cutting conditions on surface roughness of machined parts in CO2 laser cutting of pure titanium. Mater Today Proc. 2021;44:2080–6. https://doi.org/10.1016/j.matpr.2020.12.179.
16. Kochergin SA, Morgunov YA, Saushkin BP. Particularities of pulse laser cutting of thin plate titanium blanks. Procedia Eng. 2017;206:1161–6. https://doi.org/10.1016/j.proeng.2017.10.611.
17. Muzammil M, Chandra A, Kankar PK, Kumar H. Recent advances in mechanical engineering: select proceedings of ITME 2019. 1st ed. Lecture notes in mechanical engineering. Singapore: Springer; 2021. https://doi.org/10.1007/978-981-15-8704-7.
18. Tamilarasan A, Rajamani D. Multi-response optimization of Nd:YAG laser cutting parameters of Ti-6AL-4V superalloy sheet. J Mech Sci Technol. 2017;31(2):813–21. https://doi.org/10.1007/s12206-017-0133-1.
19. Singh T, Pandey AK. Parametric optimization in the laser cutting of titanium alloy sheet (grade-II). In: Muzammil M, Chandra A, Kankar PK, Kumar H, editors. Recent advances in mechanical engineering. Lecture notes in mechanical engineering. Singapore: Springer; 2021. p. 343–51. https://doi.org/10.1007/978-981-15-8704-7.
20. Muhammad N, Whitehead D, Boor A, Oppenlander W, Liu Z, Li L. Picosecond laser micromachining of nitinol and platinum–iridium alloy for coronary stent applications. Appl Phys A. 2012;106(3):607–17. https://doi.org/10.1007/s00339-011-6609-4.
21. Momma C, Knop U, Nolte S. Laser cutting of slotted tube coronary stents–state-of-the-art and future developments. Progr Biomed Res. 1999;4(1):39–44.
22. Mills B, Grant-Jacob JA. Lasers that learn: the interface of laser machining and machine learning. IET Optoelectron. 2021;15(5):207–24. https://doi.org/10.1049/ote2.12039.
23. Stelzer S, Mahrle A, Wetzig A, Beyer E. Experimental investigations on fusion cutting stainless steel with fiber and CO2 laser beams. Phys Procedia. 2013;41:399–404. https://doi.org/10.1016/j.phpro.2013.03.093.
24. Scintilla LD, Tricarico L. Fusion cutting of aluminum, magnesium, and titanium alloys using high-power fiber laser. Opt Eng. 2013;52(7):076115. https://doi.org/10.1117/1.OE.52.7.076115.
25. Jahani B. The effects of surface roughness on the functionality of Ti13Nb13Zr orthopedic implants. Biomed J Sci Tech Res. 2021;38(1):30058–67. https://doi.org/10.26717/BJSTR.2021.38.006104.
26. Chang H-I, Wang Y. Cell responses to surface and architecture of tissue engineering scaffolds. In: Eberli D, editor. Regenerative medicine and tissue engineering—cells and biomaterials. London: IntechOpen; 2011. https://doi.org/10.5772/21983.
27. Shalabi MM, Gortemaker A, Van't Hof MA, Jansen JA, Creugers NHJ. Implant surface roughness and bone healing: a systematic review. J Dent Res. 2006;85(6):496–500. https://doi.org/10.1177/154405910608500603.
28. Saptaji K, Gebremariam MA, Azhari MABM. Machining of biocompatible materials: a review. Int J Adv Manuf Technol. 2018;97(5–8):2255–92. https://doi.org/10.1007/s00170-018-1973-2.
29. Riveiro A, Quintero F, Boutinguiza M, Del Val J, Comesaña R, Lusquiños F, Pou J. Laser cutting: a review on the influence of assist gas. Materials. 2019;12(1):157. https://doi.org/10.3390/ma12010157.
30. Riveiro A, Quintero F, Lusquiños F, Del Val J, Comesaña R, Boutinguiza M, Pou J. Experimental study on the CO2 laser cutting of carbon fiber reinforced plastic composite. Compos A Appl Sci Manuf. 2012;43(8):1400–9. https://doi.org/10.1016/j.compositesa.2012.02.012.
31. Shanjin L, Yang W. An investigation of pulsed laser cutting of titanium alloy sheet. Opt Lasers Eng. 2006;44(10):1067–77. https://doi.org/10.1016/j.optlaseng.2005.09.003.